Link weight evolution in a network of coupled chemical oscillators

Hua Ke, Mark R. Tinsley, Aaron Steele, Fang Wang, and Kenneth Showalter
C. Eugene Bennett Department of Chemistry, West Virginia University, Morgantown, West Virginia 26506-6045, USA
(Received 22 December 2013; published 19 May 2014)

Link weight evolution is studied in a network of coupled chemical oscillators. Oscillators are perturbed by adjustments in imposed light intensity based on excitatory or inhibitory links to other oscillators undergoing excitation. Experimental and modeling studies demonstrate that the network is capable of producing sustained coordinated activity. The individual nodes of the network exhibit incoherent firing events; however, a dominant frequency can be discerned within the collective signal by Fourier analysis. The introduction of spike-timing-dependent plasticity yields a network that evolves to a stable unimodal link weight distribution.

DOI: 10.1103/PhysRevE.89.052712 PACS number(s): 87.19.lm, 05.45.Xt, 87.19.lj, 87.19.lw

I. INTRODUCTION

Neurons are the key cell type responsible for signal processing in the brain. The behavior of an individual neuron can be represented on different levels of detail [1], and many studies have focused on a single compartment approach in which the neuron is considered to be a dynamical point object [2]. Insights into basic brain function can be obtained by examining signal transmission and processing across networks of model neurons [2–4]. Networks have been constructed using a variety of neuronal models, including conductance models, such as the Hodgkin-Huxley system, and phenomenological models, such as integrate-and-fire schemes and three-state cellular automata [2,5,6]. Neural networks have also been implemented with electronic circuitry, the components of which capture many of the dynamical properties of individual neurons [7].

Here we use the photosensitive Belousov-Zhabotinsky (BZ) reaction [8] to develop a network of coupled micro-oscillators by using local light intensity to manipulate the excitability of each oscillator [9–12]. Unidirectional links between the oscillators, assigned prior to an experiment, are activated for a set period of time when an oscillator undergoes an excitation or fires. Light is projected from a spatial light modulator onto a linked oscillator, where the intensity is based on the sum of the activity of the input links. The activity of a photosensitive BZ oscillator increases with decreasing light intensity, and when the intensity is below a threshold level for a prescribed period of time, the oscillator undergoes an excitation. Each oscillator is capable of capturing both the formal aspect of a firing event, associated with the simplest models of neurons, and intrinsic processes that incorporate the chemical integration of the input signals.

Hebbian learning involves long-term potentiation and depression, leading to plasticity in the synaptic strengths between presynaptic and postsynaptic neurons [13]. Hebbian rules, however, may give rise to uncontrolled increases or decreases of synaptic weights [14]. Modifications of Hebbian learning have been proposed to generate a stable evolution of synaptic weights [15,16]. Spike-timing-dependent plasticity (STDP), a modified Hebbian learning algorithm, is based on experimentally measured changes in synaptic strengths [17], which show that potentiation and depression depend on the relative timing of presynaptic and postsynaptic firing events [14,18]. The implementation of an STDP algorithm in our chemical oscillator system produces a network that spontaneously evolves to a stable link weight distribution while simultaneously expanding the parameter range over which sustained coordinated activity is observed.

Our network of coupled chemical oscillators permits an examination of link weight evolution in a nonbiological system. Although the chemical oscillator network is only an approximation of an actual neuronal network, it exhibits sustained integrate-and-fire activity and STDP link weight adjustments, giving rise to a unimodal link weight distribution. This complex network evolution in a physical system points to the robustness of the STDP algorithm in link weight optimization.

II. METHODS

A. Experiment

The experiment utilizes a virtual spatial network of oscillators that is developed by mapping individual oscillators onto a 7×7 grid [19]. Links are established in the virtual network according to a placement algorithm prior to beginning each experiment. For each unidirectional link, both the source oscillator and direction of the link are selected at random. The distance of the destination oscillator is then selected according to a distance-dependent probability distribution [20]. We designate 80% of the links as excitatory, with the remainder being inhibitory [21]. Each link has an associated link weight l, with $l > 0$ for excitatory links and $l < 0$ for inhibitory links. Around 20 to 30 links per oscillator are assigned in a typical experiment. All links are constrained to connect to an oscillator within the virtual spatial distribution, and links from an oscillator to itself are prohibited.

Concentrations are selected so that under high-light-intensity conditions ϕ_{high} the catalyst-loaded particles of the system exhibit steady-state behavior. Reduction of the light intensity below a threshold value ϕ_{low} leads to an excitation. Behavior is initiated in the system by reducing the light intensity for 30 s on the four central oscillators, causing them to undergo an excitation. At each time step, the monitored gray level is examined to determine whether an oscillator has fired, and if so, the links originating at that oscillator are activated for a set period of time t_l. The illumination intensity of each oscillator is updated at each time step according to the

following rules:

$$\phi_0 - \sum_{\text{active}} l < 0 \rightarrow \ \phi = \phi_{\text{low}}, \tag{1}$$

$$\phi_0 - \sum_{\text{active}} l \geqslant 0 \rightarrow \ \phi = \phi_{\text{high}}, \tag{2}$$

where $\phi_{\text{low}} = 0.081$ mW cm^{-2} and $\phi_{\text{high}} = 1.38$ mW cm^{-2}. The summation is carried out over all currently active links using the current weight of each link.

B. Numerical model

Simulations are carried out using the two-variable Oregonator model for the photosensitive BZ reaction to represent the chemical reaction of each oscillator [22,23],

$$\frac{du_j}{dt} = \frac{1}{\epsilon}\left(u_j - u_j^2 - (\phi_j + f v_j)\frac{(u_j - q)}{u_j + q}\right), \tag{3}$$

$$\frac{dv_j}{dt} = u_j - v_j, \tag{4}$$

where u_j and v_j are the dimensionless concentrations of $HBrO_2$ and $Ru(bpy_3)^{3+}$ [tris(bipyridine)ruthenium(III)] on particle j and ϕ_j represents the rate of bromide production due to the irradiation of the particle [24]. Typical simulations involve virtual grids of up to 30×30 oscillators. The network of links is established using the same placement algorithm as in the experimental system. Model parameters are chosen so that each oscillator is in a steady state for $\phi = \phi_0$. Reduction of the light intensity below a threshold value, $\phi = 0.02$ for the parameters utilized, leads to an excitation.

III. NETWORK DYNAMICS

Sustained activity on the network is exhibited in both the experiments and simulations following an initial perturbation. Figure 1 shows a patchy wave of activity that propagates from the center of the medium, reflects from the boundary, and eventually fills the network with what appears to be asynchronous spatiotemporal structures. The likelihood of an initial perturbation propagating and producing persistent activity is dependent on the characteristics of the oscillators and the parameters associated with the network, including the intrinsic chemical time scale, number of nodes, lifetime of excitation, and weight of the links. At low values of link weight and link number, the initial perturbation dies out quickly, with the system returning to the quiescent steady state. At intermediate values, activity spreads from the initiation at the center of the system, as shown in Fig. 1.

Two illumination algorithms have been investigated in the simulations, the discrete state algorithm used in the experiments, Eqs. (1) and (2), and a continuous illumination algorithm given by $\phi = \phi_0 - \sum_{\text{active}} l$, where ϕ is prohibited from becoming negative. Both algorithms produce the same qualitative behavior, as illustrated in Fig. 2, which shows the probability of sustained activity as a function of link weight. With uniform link weights throughout the network, a sharp transition to sustained activity with increasing link weight is observed (red line with stars). When the STDP algorithm is applied (discussed below), the transition is more gradual (blue line with circles). The behavior is essentially the same with the discrete and continuous illumination algorithms except for small quantitative differences, and we therefore use the continuous algorithm to illustrate the network dynamics in our simulations.

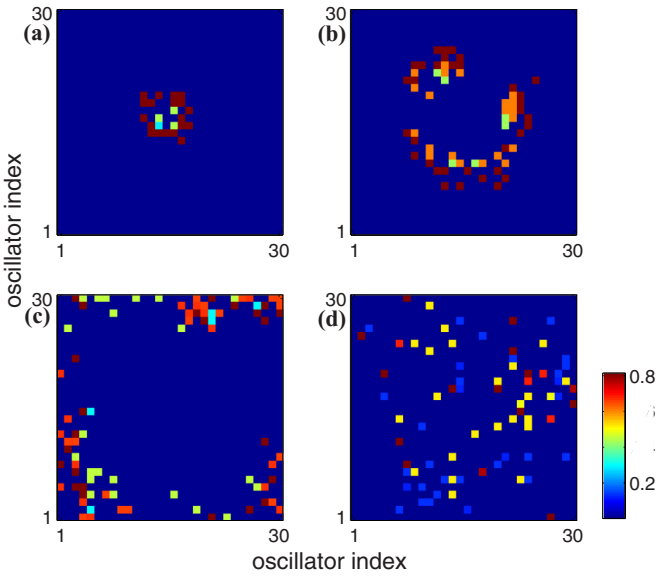

FIG. 1. (Color online) The development of activity in a chemical oscillator network simulated with the Oregonator model of the photosensitive Belousov-Zhabotinsky (BZ) reaction. Following (a) an initial perturbation at the center of the network, (b) activity spreads outward, and (c) eventually reaches the boundary of the network. Oppositely directed links initiate activity of oscillators that did not fire during the initial spread of activity. (d) These oscillators then reexcite other oscillators, leading to an aperiodic activation pattern. The probability of a link at distance r is given by $\frac{1}{\sigma\sqrt{2\pi}} e^{\frac{-r^2}{2\sigma^2}}$. System parameters are $\epsilon = 0.01$, $f = 1.4$, $q = 0.002$, number of oscillators $= 30 \times 30$, number of links $= 22{,}500$, $t_l = 2.0$, $\sigma = 2.0$ (excitatory), $\sigma = 4.0$ (inhibitory), $l = 0.04$ (excitatory), $l = -0.08$ (inhibitory), $\phi_0 = 0.15$, oscillator period $= 4.0$. The period of the oscillators is determined by reducing ϕ until the system is oscillatory (0 in simulations and 0.081 mW cm^{-2} in experiments) and measuring the frequency of each oscillator. All numerical integrations are carried out using a time step of 0.001. Activity is initiated in the network by reducing ϕ to zero on the nine central oscillators for a period of 0.25 (250 time steps). The snapshots in (a)–(d) are at $t = 0.37$, 0.85, 1.75, and 3.25, respectively, and the color scale is proportional to the dimensionless concentration v_j of the oxidized catalyst, $Ru(bpy_3)^{3+}$.

Features of the network during sustained activity are illustrated in Fig. 3. Figures 3(a) and 3(c) show typical firing patterns of the individual oscillators within the experimental and simulated networks, respectively. In both cases, the firing is irregular, with intermittent quiescent periods and periods of regular firing, giving rise to aperiodic oscillations in the global signal. Figures 3(b) and 3(d) illustrate the global behavior of the experimental and simulated networks, where the network oscillator activity is plotted as a function of time. The Fourier power spectra, shown in the insets, reveal the presence of a dominant frequency in each of these time series. In the case of the experimental system, the reciprocal of the dominant frequency is 84 s, compared to the mean

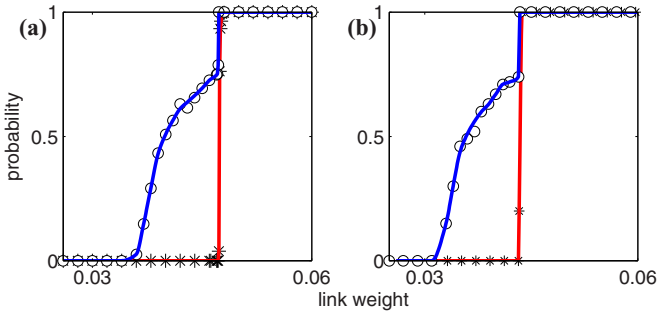

FIG. 2. (Color online) Probability of sustained activity as a function of the excitatory link weight in simulations using (a) the discrete illumination algorithm, Eqs. (1) and (2), and (b) the continuous algorithm, $\phi = \phi_0 - \sum_{\text{active}} l$. The red line with stars shows the behavior for constant, uniform link weights; the blue line with circles shows the behavior when the STDP algorithm is applied. Activity is initiated in the network by reducing ϕ to zero on the 49 central particles for a period of 0.25 (250 time steps). All probabilities are based on 500 simulations, each with a different link distribution, for each link weight. The activity is determined to be sustained if it survives for $t \geqslant 1000$. System parameters are $t_l = 1.2$, $c_d = 0.2$, $c_p = 0.019$, $\tau_0 = 0.2$. Other parameters are as in Fig. 1.

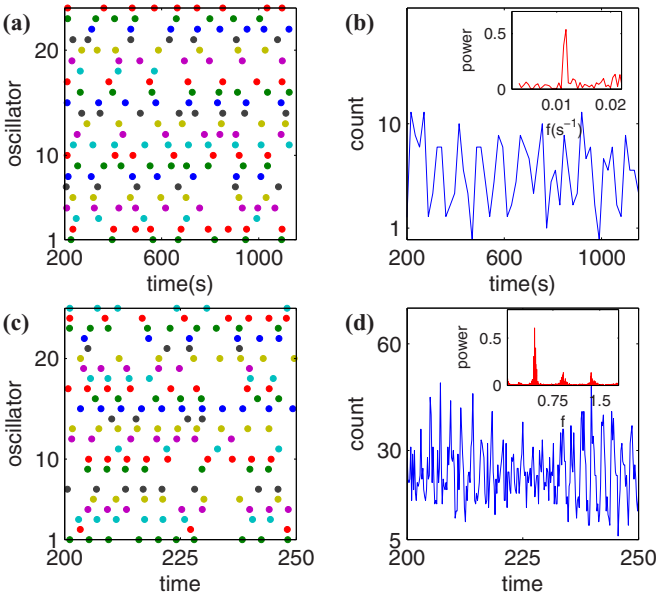

FIG. 3. (Color online) (a) Firing pattern of the experimental BZ oscillator network, showing 25 of the 49 oscillators. Each color-coded point indicates the time at which an individual oscillator fires. (b) Time series showing the number of oscillators that fire in a given interval of time. The count is constructed by binning the time series into intervals of 9 s and determining the number of firing oscillators in each interval. The inset shows the power spectrum of the time series. The probability of a link at distance r is given by $\frac{1}{\sigma\sqrt{2\pi}} e^{\frac{-r^2}{2\sigma^2}}$. System parameters are number of particles $= 7 \times 7$, number of links $= 980$, $t_l = 80$ s, mean period $= 120$ s, $\sigma = 2.0$ (excitatory), $\sigma = 4.0$ (inhibitory), $l = 0.04$ (excitatory), $l = -0.08$ (inhibitory). Other parameters are as in Ref. [19]. (c) Firing pattern of the simulated BZ oscillator network, showing 25 of the 900 oscillators. (d) Time series showing the number of oscillators that fire in a given interval of time (interval $= 0.2$). The inset shows the power spectrum of the time series. Other parameters are as in Fig. 1.

period of the oscillators of 120 s, while in the simulations, the reciprocal of the dominant frequency is 2.1 compared to the mean period of 4.0. While we do not expect the two-variable Oregonator model to quantitatively match the experimental behavior, we see in both cases that the fundamental frequency associated with the global signal is significantly higher than the frequencies of the component oscillators. The fundamental frequency appears to arise from the overall rate of different nodes firing at any moment throughout the network.

Link weight evolution in the network can be investigated by incorporating an algorithm for STDP into the model. The STDP algorithm makes an adjustment of the link weight between two neurons based on their relative firing times. The time difference between the firing of the presynaptic neuron and the postsynaptic neuron is given by $\Delta t = t_{\text{post}} - t_{\text{pre}}$. Hebbian link weight changes take place primarily for small values of Δt, according to

$$w_t = w_{t-1} + c_p e^{-\Delta t/\tau_0}, \tag{5}$$

$$w_t = w_{t-1} - c_d w_{t-1} e^{\Delta t/\tau_0}, \tag{6}$$

where c_p and c_d are the potentiation and depression parameters, respectively, that scale the changes in the link weight [14]. Potentiation occurs only for positive Δt, Eq. (5), and depression occurs only for negative values of Δt, Eq. (6). The time scale for the impact of the STDP is determined by τ_0. The weight-dependent adjustment in Eq. (6) gives rise to a stable distribution of link weights [14]. Models of STDP in which the adjustment of the depression link weight does not depend on the current link weight often result in bimodal distributions. The inclusion of link-weight-dependent depression gives rise to unimodal distributions by reducing heavily weighted links rapidly while only slightly reducing weak links. The STDP algorithm is applied only to excitatory links, with inhibitory links assumed to remain at constant strength.

The evolution of the link weight distribution in the experimental oscillator network has been characterized, and an example of the distribution at successive times is shown in Fig. 4(a). In this experiment, all of the excitatory links have a uniform initial value of $l = 0.04$. The STDP algorithm is applied for the duration of the experiment, and the distribution of excitatory link weights evolves to eventually produce a distribution with a mean value of $l = 0.055$. The long-term behavior associated with this algorithm can be explored further with the computational model. Starting with a system in which $l = 0.045$ for all of the excitatory links, the application of the STDP algorithm leads to a gradual increase in the mean value of the link weights. The resulting stable, slightly skewed distribution is shown in Fig. 4(b). For the same set of parameters, but with a higher initial excitatory link weight, $l = 0.12$, the mean link weight now slowly decreases to eventually produce the stable, slightly skewed distribution shown in Fig. 4(c). The two final distributions are virtually the same, with almost identical mean values and overall shapes. The inset in Fig. 4(b) shows the mean value of the link weights of the two distributions as a function of time, which converge to the same value of 0.11.

A necessary condition for an STDP algorithm to produce a stable distribution of link weights is that coordinated activity

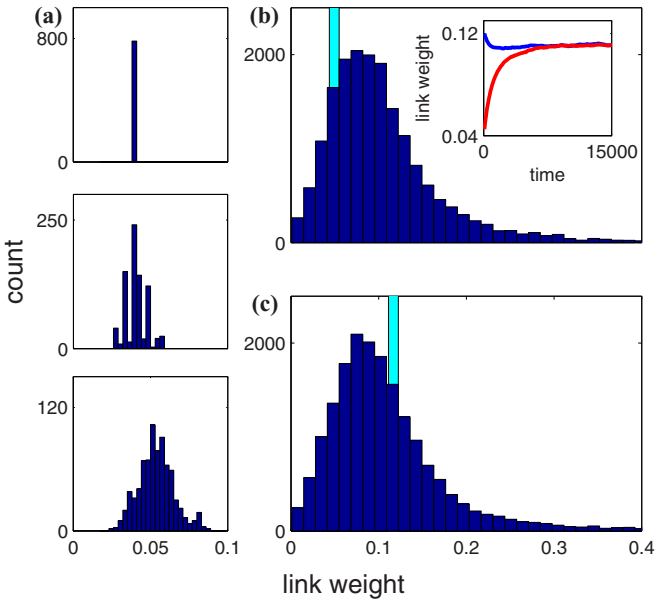

FIG. 4. (Color online) (a) Evolution of link weight distribution with the STDP algorithm applied in the experimental BZ oscillator network. Link distribution at times (top) 0 s, (middle) 600 s, and (bottom) 1500 s. System parameters are $t_l = 60$ s, $c_d = 0.15$, $c_p = 0.01$, $\tau_0 = 120$ s. All other parameters are as in Fig. 3. Evolution of link weight distribution with the STDP algorithm applied in the model BZ oscillator network: (b) Initial link weight = 0.045 [light blue (light gray)] and link weight distribution at time 15 000 [dark blue (dark gray)]. (c) Initial link weight = 0.120 [light blue (light gray)] and link weight distribution at time 15 000 [dark blue (dark gray)]. The inset in (b) shows the temporal evolution of the mean link weight for the simulations in (b) [red (light gray)] and (c) [dark blue (dark gray)]. Other parameters are as in Fig. 1.

on the network is sustained. Following an initial perturbation, sustained coordinated activity is observed once the mean excitatory link weight evolves above, or is initially above, a critical threshold. The impact of allowing the link weights to evolve according to the STDP algorithm is shown in Fig. 2. In this case, the link weight values of the abscissa correspond to the initial uniform excitatory link weight, as in the simulations shown in Figs. 4(b) and 4(c). A significant fraction of the simulations exhibit sustained activity with an initial link weight below 0.047, the critical transition link weight for the constant link weight simulations. The expansion of the region in which sustained activity is observed can be understood by examining Fig. 4(b), in which the initial link weight is below the critical threshold for sustained activity. Provided that the system continues to evolve by the STDP algorithm, the mean link weight distribution will increase above the critical threshold value associated with sustained activity. Realizations that fail to sustain activity correspond to those that collapse prior to the mean link weight attaining or exceeding this critical value. Figure 4 also demonstrates that the system has a well-defined, unimodal link weight distribution as an attractor. Networks with a low initial link weight, as in Fig. 4(b), or a high initial link weight, as in Fig. 4(c), converge to the same attractor.

IV. DISCUSSION

We have studied a network of chemical oscillators in which the coupling occurs according to a feedback algorithm that determines the intensity of illumination of a particular oscillator and thereby its excitability. The input to the feedback algorithm is the transmitted light intensity of each oscillator that is linked to the illuminated oscillator, which provides information on whether the linked oscillator has fired. This information is used in an integrate-and-fire algorithm to calculate whether an input threshold has been reached, and if so, the illumination intensity generated by the spatial light modulator is reduced. If the oscillator fires, the timing of the firing is compared with the firing time of each of the linked oscillators to adjust the link weights according to a STDP algorithm. This process leads to continuous link weight adjustments and an evolution of the link weight distribution. The chemical oscillator network is only an approximation of an actual neuronal network; however, this remarkably complex physical network demonstrates link weight evolution based on chemical oscillator integrate-and-fire dynamics and STDP link weight adjustments. The obvious dynamical differences between chemical oscillators and neurons as well as the difference in size of the relatively small chemical oscillator network compared to an actual neuronal network suggest an intrinsic robustness of the STDP algorithm for network evolution.

A recent study of two pulse-coupled chemical oscillators [25,26], with time-delayed excitatory and inhibitory coupling, reported in-phase and antiphase synchronization that is strongly dependent on the mode of coupling. The chemical oscillator network described here shares many of these features, including a form of delayed pulse coupling in the integrate-and-fire mechanism. A recent study of a model neuronal network with STDP found rapid irregular oscillations superimposed on slow collective oscillations [27]. These slow oscillations were explained by the *Sisyphus effect*, which arises from the continual readjustment of the link weights in the network by the STDP algorithm. In the chemical oscillator network described here, an evolution of the link weights to a stable unimodal distribution was found rather than an oscillatory distribution. We will investigate the differences in the networks that give rise to these differences in link weight evolution in future studies.

ACKNOWLEDGMENT

This material is based on work supported by the National Science Foundation (Grant No. CHE-1212558).

[1] M. Hines and N. Carnevale, Neural Comput. **9**, 1179 (1997).
[2] R. Brette, M. Rudolph, T. Carnevale, M. Hines, D. Beeman, J. M. Bower, M. Diesmann *et al.*, J. Computational Neurosci. **23**, 349 (2007).
[3] A. N. Burkitt, Biol. Cybern. **95**, 97 (2006).
[4] E. Izhikevich, Int. J. Bifurcation Chaos Appl. Sci. Eng. **10**, 1171 (2000).
[5] A. Roxin, H. Riecke, and S. A. Solla, Phys. Rev. Lett. **92**, 198101 (2004).

[6] G. C. Garcia, A. Lesne, M.-T. Hütt, and C. C. Hilgetag, Front. Comput. Neurosci. **6**, 50 (2012).
[7] J. Hopfield and D. Tank, Science **233**, 625 (1986).
[8] A. N. Zaikin and A. M. Zhabotinsky, Nature (London) **225**, 535 (1970).
[9] R. Toth and A. F. Taylor, Prog. React. Kinet. Mech. **31**, 59 (2006).
[10] A. F. Taylor, P. Kapetanopoulos, B. J. Whitaker, R. Toth, L. Bull, and M. R. Tinsley, Phys. Rev. Lett. **100**, 214101 (2008).
[11] M. R. Tinsley, S. Nkomo, and K. Showalter, Nat. Phys. **8**, 662 (2012).
[12] S. Nkomo, M. R. Tinsley, and K. Showalter, Phys. Rev. Lett. **110**, 244102 (2013).
[13] G. G. Turrigiano and S. B. Nelson, Nat. Rev. Neurosci. **5**, 97 (2004).
[14] M. C. W. van Rossum, G. Q. Bi, and G. G. Turrigiano, J. Neurosci. **20**, 8812 (2000).
[15] L. F. Abbott and S. B. Nelson, Nat. Neurosci. **3**, 1178 (2000).
[16] A. Morrison, M. Diesmann, and W. Gerstner, Biol. Cybern. **98**, 459 (2008).
[17] H. Markram, Science **275**, 213 (1997).
[18] R. C. Froemke and Y. Dan, Nature (London) **416**, 433 (2002).
[19] Experiments are carried out with photosensitive BZ micro-oscillators, which are illuminated at intensities that are algorithmically determined [9–12]. The oscillator particles are cation exchange beads, with diameters of 100–200 μm, that are loaded with the $[Ru(bpy)_3]^{2+}$ catalyst of the photosensitive BZ reaction. The particles are placed in a bath of continually refreshed, catalyst-free BZ solution of 0.166 M $NaBrO_3$, 0.054 M malonic acid, 0.162 M bromomalonic acid, and 0.366 M H_2SO_4. A CCD camera records the position and transmitted light intensity of each particle. Images of the reaction domain are obtained with the projected background light, $\phi_0 = 0.27$ mW cm^{-2}. A half mirror reflects the projected image from the spatial light modulator to the reaction domain, while permitting transmitted light intensity measurements with the CCD camera. Typical experiments involve 49 oscillators, and images are captured every 2 s.
[20] D. T. J. Liley, D. M. Alexander, J. J. Wright, and M. D. Aldous, Network Comput. Neural Syst. **10**, 79 (1999).
[21] B. Siri, M. Quoy, B. Delord, B. Cessac, and H. Berry, J. Physiol. (Paris) **101**, 136 (2007).
[22] R. J. Field and R. M. Noyes, J. Chem. Phys. **60**, 1877 (1974).
[23] L. Kuhnert, Nature (London) **319**, 393 (1986).
[24] S. Kádár, T. Amemiya, and K. Showalter, J. Phys. Chem. A **101**, 8200 (1997).
[25] V. Horvath, P. L. Gentili, V. K. Vanag, and I. R. Epstein, Angew. Chem. Int. Ed. **51**, 6878 (2012).
[26] M. Bär, E. Schöll, and A. Torcini, Angew. Chem. Int. Ed. **51**, 9489 (2012).
[27] K. Mikkelsen, A. Imparato, and A. Torcini, Phys. Rev. Lett. **110**, 208101 (2013).